



## Engineering polarization entanglement at telecom wavelengths

Florian Kaiser, Amandine Issautier, Lutfi Arif Ngah, Olivier Alibart, Anthony Martin, Sébastien Tanzilli

### ► To cite this version:

Florian Kaiser, Amandine Issautier, Lutfi Arif Ngah, Olivier Alibart, Anthony Martin, et al.. Engineering polarization entanglement at telecom wavelengths. Frontiers in Optics (FIO'12), Oct 2012, Rochester, United States. hal-00847653

**HAL Id: hal-00847653**

**<https://hal.science/hal-00847653>**

Submitted on 24 Jul 2013

**HAL** is a multi-disciplinary open access archive for the deposit and dissemination of scientific research documents, whether they are published or not. The documents may come from teaching and research institutions in France or abroad, or from public or private research centers.

L'archive ouverte pluridisciplinaire **HAL**, est destinée au dépôt et à la diffusion de documents scientifiques de niveau recherche, publiés ou non, émanant des établissements d'enseignement et de recherche français ou étrangers, des laboratoires publics ou privés.

# Engineering polarization entanglement at telecom wavelengths

F. Kaiser, A. Issautier, L. A. Ngah, O. Alibart, A. Martin\*, and S. Tanzilli

Laboratoire de Physique de la Matière Condensée, CNRS UMR 7336, Université de Nice - Sophia Antipolis, France  
sebastien.tanzilli@unice.fr, \*Currently with the Group of Applied Physics, Uni. Geneva (CH)

**Abstract:** We report a versatile guided-wave approach for engineering high-quality polarization entanglement at telecom wavelengths. This scheme enables manipulating photonic bandwidths ranging from 25 MHz to 1 THz, and creating any two-photon state.

**OCIS codes:** 270.5565, 060.5565, 190.4390.

## 1. Entanglement for quantum network applications at telecom wavelengths

Entanglement is a key resource for fundamental tests of quantum physics as well as for modern quantum information protocols [1], including quantum cryptography [2], quantum relays [3] and repeaters [4].

The association of standard low-loss optical fibers and reliable guided-wave components make it possible to create and distribute photonic entanglement in the telecom C-band of wavelengths (1530-1565 nm). In addition, entanglement can be easily produced by spontaneous parametric down-conversion (SPDC) in nonlinear crystals. Usual observables are time-bin and polarization, the latter being easier to manipulate, thanks to simple experimental apparatus, real-time fiber birefringence compensation, and the natural design of heralded quantum memories for this observable [5].

Today's quantum network applications follow two main routes. On one hand, utilizing the full spectral bandwidth of the paired photons created by SPDC enables dense wavelength division multiplexed (WDM) quantum cryptography [2]. On the other hand, adapting the photonic spectral bandwidths to the absorption bandwidths of currently developed quantum memory devices opens the way to quantum storage applications. More specifically here, telecom photons are used to create and distribute, and quantum memories to store, entanglement [4]. Compared to the  $\sim 1$  THz bandwidth generally available from SPDC, quantum memory spectral acceptances range from a few MHz (cold atoms [5, 6]) to a few GHz (solid-state devices [7, 8] or hot atomic vapors [9]).

In the following, we discuss a versatile polarization entangling scheme based on a birefringent delay line (BDL) that can be applied to photon bandwidths ranging from 25 MHz to 1 THz. We demonstrate such a versatility by violating, by large amounts, the Bell inequalities for 3 different bandwidths: 25 MHz, 500 MHz, and 100 GHz.

## 2. A fully guided-wave approach towards manipulating polarization two-photon states

### 2.1. Engineering polarization entangled states using a fiber birefringence delay line

The setup of the source is shown in Fig. 1.

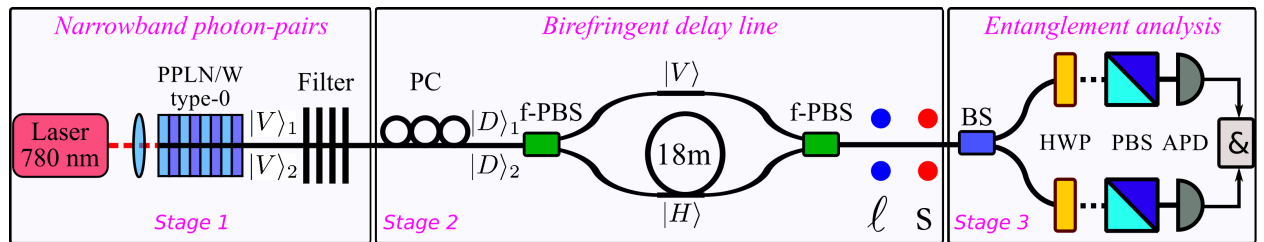


Fig. 1. Experimental setup. Starting with a waveguide photon-pair generator, the spectral bandwidth can be chosen at will using a filter (stage 1). Polarization entanglement is engineered using a BDL (stage 2). The entanglement quality is measured with a standard Bell test apparatus (stage 3) oriented in the diagonal basis for the measurement results presented in Fig. 2 [10].

A highly efficient type-0 PPLN waveguide is pumped by a stabilized 780 nm laser (stage 1). Here, vertically polarized ( $|V_1, V_2\rangle$ ) paired photons are produced by SPDC at 1560 nm, and collected by a single mode fibre. At this stage no polarization entanglement is available. In order to engineer entanglement, the paired photons are rotated to diagonal states ( $|D_1, D_2\rangle$ ) using a polarization controller (PC) and sent to the BDL (stage 2). More precisely, the  $|D_1, D_2\rangle$  paired photons are sent to an actively stabilised unbalanced Mach-Zehnder interferometer arrangement made of two fiber polarising beam splitters (f-PBS) and polarization maintaining fibers. In this particular realisation, the path length difference is of 18 m, meaning that the  $|H\rangle$  polarization component is delayed by 76 ns compared to the  $|V\rangle$  counterpart. Via

post-selection of simultaneously exiting photons, the polarization entangled state  $|\Phi(\phi)\rangle = \frac{1}{\sqrt{2}}(|H_1, H_2\rangle + e^{i\phi}|V_1, V_2\rangle)$  is obtained. More generally, note that the probability amplitudes and the phase  $\phi$  of the state are easily accessible by controlling the input polarization state and by fine tuning of the fiber length of the BDL, respectively. Therefore, any state of the form  $\alpha|H_1, H_2\rangle + e^{i\phi}\beta|V_1, V_2\rangle$  can be achieved, including the four maximally entangled Bell states.

## 2.2. Key features of the source

The time separation of 76 ns between the  $|H, H\rangle$  and  $|V, V\rangle$  components of the state enables filtering the paired photons down to a bandwidth of 25 MHz, which corresponds to a coherence time of 18 ns. This makes our configuration versatile in the sense that the bandwidth can be chosen at will between 25 MHz and 2 THz (natural emission bandwidth of our crystal). To demonstrate this versatility, we take advantage of 3 different filters, *i.e.* of 100 GHz (standard telecom-channel WDM), 540 MHz, and 25 MHz. The first filter is rather broad, but can be advantageously utilized for dense-WDM quantum cryptography applications. The two narrower ones are adapted to quantum storage, since they match the absorption bandwidths of some solid-state ( $\sim 100$  MHz) and cold-atom ( $\sim 10$  MHz) based quantum memories, respectively. Note that these are phase-shifted fiber Bragg grating filters.

## 2.3. Measured entanglement quality and brightness

The source quality is measured by violating the Bell inequalities using a standard apparatus (half waveplate + PBS (stage 3)). As shown in Fig. 2, net visibilities close to unity ( $> 99\%$ ) are obtained, for the 3 filters, when the measurement apparatus is set in the diagonal basis and the phase  $\phi$  in the BDL is scanned over  $2\pi$ . These results are signatures of very high-quality entangled states and indicate the relevance of our approach. Moreover, the brightness achieved with this source is of  $\sim 300$  pairs created/(s  $\cdot$  mW  $\cdot$  MHz), which stands for, together with the entanglement quality, to a new state-of-the-art reference [10].

To render the source compatible with current quantum memories, the wavelength of the photons can be converted coherently from the telecom to the visible range [6, 11], where most quantum memories operate. Our approach should therefore play an important role in future quantum network applications combining telecom photons, quantum memories, and, depending on the memory devices, wavelength converters. With broader bandwidths ( $\sim 100$  GHz), our source can also be applied to dense-WDM, entanglement-based, quantum cryptography using the standard ITU telecom channels. Eventually, this source is also versatile in the sense that it can produce any of the four Bell states using the phase control in the BDL and an additional half waveplate placed on the path of one of the output photons.

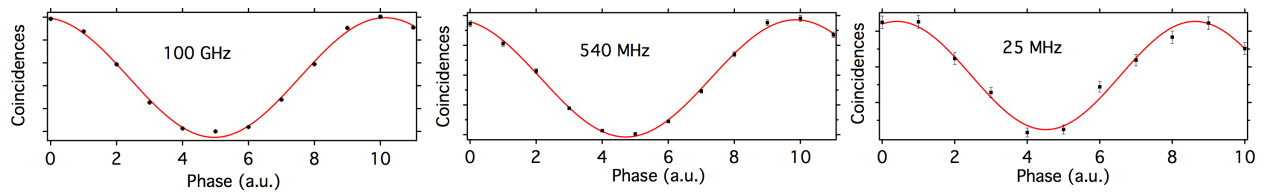


Fig. 2. Violations of the Bell inequalities when performing a phase scan in the diagonal basis showing  $V_{net} > 99\%$  for the 3 filters. Note that comparable visibilities are also obtained when performing standard Bell inequality measurements for the polarization observable [10].

## References

1. W. Tittel and G. Weihs, *Quant. Inf. Comp.* **1**, 3 (2001).
2. N. Gisin *et al.*, *Rev. Mod. Phys.* **74**, 145 (2002).
3. P. Aboussouan *et al.*, *Phys. Rev. A* **81**, 021801(R) (2010).
4. N. Sangouard *et al.*, *Rev. Mod. Phys.*, **83**, 33 (2011).
5. H. Tanji *et al.*, *Phys. Rev. Lett.* **103**, 043601 (2009).
6. Y. O. Dudin *et al.*, *Phys. Rev. Lett.* **105**, 260502 (2010).
7. C. Clausen *et al.*, *Nature* **469**, 508–511 (2011).
8. E. Saglamyurek *et al.*, *Nature* **469**, 512–515 (2011).
9. K. F. Reim *et al.*, *Nature Photon.* **4**, 218 (2010).
10. F. Kaiser *et al.*, arXiv:1111.5683 (2012).
11. S. Tanzilli *et al.*, *Nature*, **437**, 116 (2005).